UvA-DARE (Digital Academic Repository)

Non-Fermi-liquid scaling in heavy-fermion UCu3.5 Al1.5 and UCu3Al2

Nakotte, H.; Prokes, K.; Bruck, E.H.; Buschow, K.H.J.; de Boer, F.R.; Andreev, A.V.; Aronson, M.C.; Lacerda, A.; Torikachvili, M.; Robinson, R.A.; Bourke, M.A.M.; Schultz, A.J.

Non-Fermi-liquid scaling in heavy-fermion UCu$_{3.5}$Al$_{1.5}$ and UCu$_3$Al$_2$

H. Nakotte

Manuel Lujan Jr. Neutron Scattering Center, Los Alamos National Laboratory, Los Alamos, New Mexico 87545

K. Prokeš, E. Brück, K. H. J. Buschow, and F. R. de Boer

Van der Waals-Zeeman Institute, University of Amsterdam, Valckenierstraat 65, 1018 XE Amsterdam, The Netherlands

A. V. Andreev

Institute of Physics, Academy of Sciences, Na Slovance 2, 18 040 Prague 8, The Czech Republic

M. C. Aronson

The Harrison M. Randall Laboratory of Physics, University of Michigan, Ann Arbor, Michigan 48109-1120

A. Lacerda

National High Magnetic Field Laboratory, Pulsed Field Facility, Los Alamos National Laboratory, Los Alamos, New Mexico 87545

M. S. Torikachvili

Department of Physics, San Diego State University, San Diego, California 92182

R. A. Robinson and M. A. M. Bourke

Manuel Lujan Jr. Neutron Scattering Center, Los Alamos National Laboratory, Los Alamos, New Mexico 87545

A. J. Schultz

Intense Pulsed Neutron Source, Argonne National Laboratory, Argonne, Illinois 60439-4814

We report on specific-heat, magnetic-susceptibility, high-field-magnetization, electrical-resistivity, and neutron-diffraction results on UCu$_{3.5}$Al$_{1.5}$ (polycrystal) and UCu$_3$Al$_2$ (polycrystal and single crystal). Our results indicate that both compounds crystallize in the hexagonal CaCu$_5$ structure with ordered UCu$_2$ planes separated by planes containing a statistical distribution of Al along with the remaining Cu atoms. At low temperatures, the specific heat and the magnetic susceptibility of both compounds are enhanced, but their temperature dependences are found to be distinct from expectations of Fermi-liquid theory. UCu$_{3.5}$Al$_{1.5}$ does not order magnetically, and the low-temperature specific heat and magnetic susceptibility show scaling behavior ($C/T \propto \ln T$ and $\chi \propto T^{-1/3}$) reminiscent of non-Fermi-liquid materials. For UCu$_3$Al$_2$, on the other hand, the low-temperature scaling of bulk properties is masked by an anomaly around 8–10 K, which is presumably of magnetic origin. Single-crystal studies of UCu$_3$Al$_2$ reveal a huge magnetic anisotropy with very different in-plane response compared to the c-axis response. Our data provide evidence that any temperature dependence of the magnetic susceptibility (and electrical resistivity) of polycrystalline material may be due to averaging anisotropic response over all crystallographic directions. The results are discussed in the context of findings from other non-Fermi-liquid materials. [S0163-1829(96)04641-3]

I. INTRODUCTION

Heavy-fermion behavior found in a number of Ce-, Yb-, and U-based compounds has been studied extensively for almost two decades. For most heavy-fermion materials, the low-temperature properties are well described in terms of Fermi-liquid theory.[1] In the limit $T \to 0$, the Fermi-liquid theory predicts large contributions to the specific heat ($= \gamma T$), the Pauli-like spin susceptibility ($= \chi_0$), and the electrical resistivity ($= AT^2$) with temperature-independent parameters γ, χ_0, and A. In general, heavy-fermion behavior may occur due to two different mechanisms: (a) the ''screening'' of a magnetic moment due to the Kondo effect and (b) magnetic-correlation effects. The former mechanism causes

mass renormalization in a local-moment system, and the latter mechanism is applied to bandlike magnets (itinerant magnetism). Most heavy-fermion compounds are located at the borderline between local-moment and itinerant magnetism, and it is on that borderline where deviations from the Fermi-liquid behavior may be found. Recently, a number of materials, which display the so-called ''non-Fermi-liquid behavior,'' have attracted much attention.[1–3] The hallmark for non-Fermi-liquid behavior is a divergence in the specific heat, i.e., $C/T \propto -\ln(T/T_0)$, but divergences are also expected in other bulk properties.

Up to now, non-Fermi-liquid behavior was achieved mainly in dilute systems,[2,3] where some kind of disorder is introduced onto the crystal lattice. The role of disorder dif-

fers for the various scenarios (ranging from single-ion two-channel Kondo mechanism to collective effects) proposed for the occurrence of non-Fermi-liquid behavior.

The presently known non-Fermi-liquid materials fall into two categories: (a) the f-electron sublattice is diluted, and (b) the f-ion sublattice is kept intact, but its surrounding is changed by controlled substitutions. Examples of the former category are $(U,Y)Pd_3$ compounds[4,5] and the $(U,Th)Ru_2Si_2$ system,[6] while $Ce(Cu,Au)_6$ compounds[7] and $U(Cu,Pd)_5$ representatives[8] fall in the latter category. Non-Fermi-liquid scaling has been proposed for some compositions in all of the above systems, though sometimes different mechanisms have been proposed for its occurrence. Furthermore, while a logarithmic divergence of the specific heat is common to all of the above systems, quite different scaling behavior has been found in other bulk properties. Perhaps the strongest evidence for non-Fermi-liquid behavior has been found in $UCu_{3.5}Pd_{1.5}$ and UCu_4Pd, where inelastic-neutron-scattering experiments[9] provide evidence for universal scaling of the dynamical susceptibility below 25 meV. The scale invariance in the $U(Cu,Pd)_5$ system suggests that a $T=0$ phase transition is responsible for non-Fermi-liquid scaling in $UCu_{3.5}Pd_{1.5}$ and UCu_4Pd.

Recently, we have reported on the large enhancements in the low-temperature specific heat of a number of UCu_xAl_{5-x} compounds,[10] but little consideration was given to the origin of such enhancements. In the present paper, we argue whether the bulk properties of two members of this family, namely, $UCu_{3.5}Al_{1.5}$ and UCu_3Al_2, display a temperature behavior expected for non-Fermi-liquid materials.

In contrast to the cubic $U(Cu,Pd)_5$ compounds, UCu_xAl_{5-x} compounds crystallize in the hexagonal $CaCu_5$ structure for $2.9 \leq x \leq 3.5$. Therefore, magnetic (and transport) properties are expected to be anisotropic. Single-crystal studies of UCu_3Al_2 indeed reveal a huge magnetic anisotropy,[11] and its consequences will be discussed here. For this compound, antiferromagnetic ordering below 8–10 K has been suggested on the basis of anomalies of the bulk properties at this temperature.[10,11]

Our previous neutron-diffraction studies[11] revealed that for UCu_3Al_2 the U atoms occupy the $1a$ positions of the $CaCu_5$ structure and the $2c$ positions are occupied by Cu atoms only, while a random distribution of Cu and Al atoms is found on the $3g$ sites. The resultant structure, which is the same as reported for the two heavy-fermion superconductors UNi_2Al_3 and UPd_2Al_3,[12] is shown in Fig. 1 and the structural parameters are given in Table I. Therefore, in UCu_3Al_2, perfectly ordered UCu_2 planes are separated by planes of statistically distributed Cu and Al atoms which exist in a *Kagomé* net.[13] Using x-ray diffraction, Blažina and Ban[14] have proposed that $UCu_{3.5}Al_{1.5}$ also adopts the above structure. This, however, seems to be in contrast to our observation that, even in the composition range $2.9 \leq x \leq 3.5$, some UCu_xAl_{5-x} syntheses do not form as a single phase.[10] For $UCu_{3.3}Al_{1.7}$, we found two $CaCu_5$-type phases with entirely different lattice parameters (see Fig. 2). We have argued that slight structural modifications may occur in this composition range (e.g., complete disorder of Cu/Al for $x > 3.3$ as opposed to marginal disorder for $x < 3.3$). To clarify this issue, we decided to verify the crystal structure of $UCu_{3.5}Al_{1.5}$ by neutron powder diffraction.
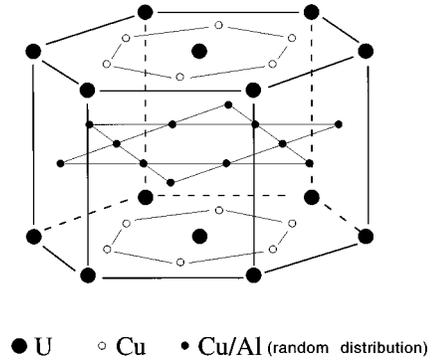

● U   ○ Cu   • Cu/Al (random distribution)

FIG. 1. Schematic drawing of the crystal structure of UCu_3Al_2 and $UCu_{3.5}Al_{1.5}$ (hexagonal $CaCu_5$ type). Note that ordered UCu_2 planes are separated by planes of statistically distributed Al and Cu atoms which exist in a *Kagomé* net.

Finally, we also present neutron diffraction on single-crystalline UCu_3Al_2 to gain some insight regarding the magnetic ground state, i.e., to clarify the origin of the anomaly around 8–10 K which is visible in the bulk properties.

II. SAMPLE PREPARATION AND CHARACTERIZATION

Polycrystalline samples of UCu_3Al_2 and $UCu_{3.5}Al_{1.5}$ were prepared by arc melting stoichiometric amounts of the constituents with a purity of at least 99.9%. The buttons were encapsulated in quartz tubes under Ar atmosphere and were subsequently annealed for 2 months at 600 °C. For both samples, all reflections in the x-ray-diffraction patterns were found to index in the proper $CaCu_5$ structure. The absence of any unindexed peaks indicates an upper limit of impurity phases of about 5% for both samples. Electron microprobe analysis, however, revealed a small amount of a Cu-rich secondary phase in both samples, which was later identified as U_2Cu_9Al by means of neutron diffraction (see Sec. IV). The main phases, on the other hands, were found to exhibit compositions very close to the intended stoichiometry (within 3% of the elemental fractions).

In the case of UCu_3Al_2, we also tried to grow a single crystal using the Czochralski tri-arc method. We obtained an ingot, in which some almost single-crystalline parts with a small twinning were found. These ''single crystals'' were extracted from the material and subsequently annealed. Our best crystal, approximately 50 mg in mass, was checked by neutron diffraction on the Single Crystal Diffractometer (SCD) at the Intense Pulsed Neutron Source at Argonne National Laboratory. At room temperature, almost all of the observed reflections (more than 200) of that crystal were indexed in the appropriate $CaCu_5$ structure. However, we also found about 10 relatively weak unindexed reflections, which may indicate a small amount of an impurity phase to be present in the crystal. In addition, we found a large broadening for most reflections, and this prevented a determination of the distribution of Cu and Al on the $2c$ and $3g$ sites due to the poor quality of our single crystal. A closer inspection, however, showed that crystal imperfections are mainly due to a large mosaicity within the hexagonal basal plane (with an angular spread of about 5°), while the c-axis orientation is well defined. This does allow separation of the magnetic

TABLE I. Refined structural parameters of $UCu_{3.5}Al_{1.5}$ and UCu_3Al_2.

	$UCu_{3.5}Al_{1.5}$					UCu_3Al_2			
	Space group: *P6/mmm*					Space group *P6/mmm*			
	x	y	z	fraction[a]		x	y	z	fraction[a]
U(1*a*)	0	0	0	1.00	U(1*a*)	0	0	0	1.00
Cu(2*c*)	1/3	2/3	0	1.00	Cu(2*c*)	1/3	2/3	0	1.00
Cu(3*g*)	1/2	0	1/2	0.50	Cu(3*g*)	1/2	0	1/2	0.33
Al(3*g*)	1/2	0	1/2	0.50	Al(3*g*)	1/2	0	1/2	0.67
	300 K[b]	300 K	12 K			300 K[b]	300 K[c]		
	(x-ray)	(neutron)	(neutron)			(x-ray)	(neutron)		
a (Å)	5.090(4)	5.0989(1)	5.0815(1)			5.145(4)	5.1402(1)		
c (Å)	4.159(3)	4.1611(1)	4.1515(1)			4.154(3)	4.1472(1)		
Rwp		9.41%	9.11%				4.99%		
Rp		6.32%	6.13%				3.60%		
Reduced χ^2		4.768	4.093				4.698		

[a]Fractions have been fixed to the exact stoichiometry for a better comparison.
[b]X-ray data (taken from Ref. 10).
[c]Neutron data obtained at the NIST research reactor (taken from Ref. 11).

contributions to the basal-plane and *c*-axis response. The crystal was used to check the magnetic properties and for the single-crystal neutron-diffraction experiment.

III. BULK STUDIES

We studied the specific heat, the magnetic susceptibility, the high-field magnetization, and the electrical resistivity on polycrystals of $UCu_{3.5}Al_{1.5}$ and UCu_3Al_2. Furthermore, we report on the magnetic properties of single-crystalline UCu_3Al_2.

A. Specific heat

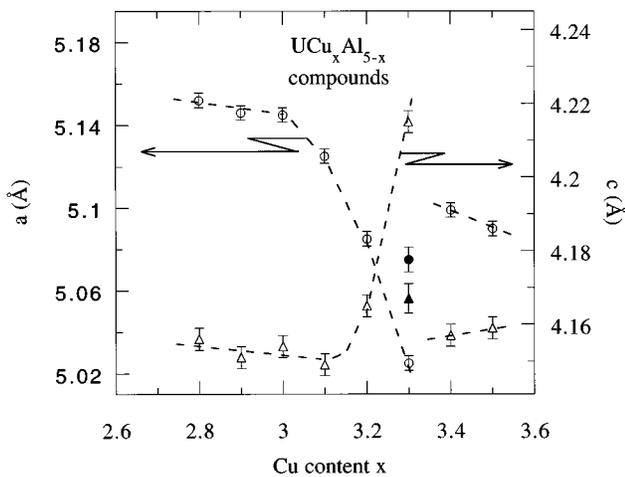Specific-heat measurements between 300 mK and 1.2 K were performed in a ^{3}He cryostat using the relaxation-time method. Between 1.2 and 50 K, the specific heat was measured using a semiadiabatic method in a different setup equipped with a superconducting 5-T coil.

The temperature dependences of the specific heat of $UCu_{3.5}Al_{1.5}$ and UCu_3Al_2 are shown in Fig. 3 as C/T vs log T. For $UCu_{3.5}Al_{1.5}$, we find a logarithmic dependence of C/T below 6 K. Such a dependence is usually taken as a signature of non-Fermi-liquid scaling.[3] The low-temperature scaling of the specific heat of UCu_3Al_2, on the other hand, is masked by a maximum, which occurs around 8 K. The maximum may indicate the onset of magnetic correlations in UCu_3Al_2 at this temperature. Above 1.2 K, there was no change in either specific heat upon application of a magnetic
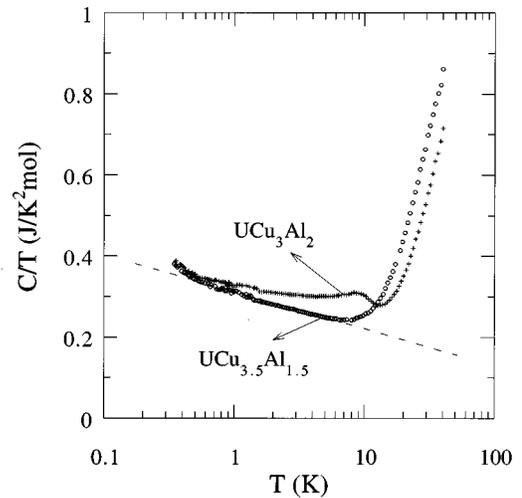

FIG. 2. Variation of the lattice parameters a (○) and c (△) vs copper content in UCu_xAl_{5-x} compounds (after Ref. 10). Note that two $CaCu_5$-type phases appear in the diffraction pattern of $UCu_{3.3}Al_{1.7}$ with different sets of lattice parameters (open and solid symbols). The lines are guides to the eye.

FIG. 3. Temperature dependence of the specific heat of $UCu_{3.5}Al_{1.5}$ (○) and UCu_3Al_2 (+). Note the logarithmic temperature scale. The dashed line is a straight-line fit to the low-temperature part of C/T of $UCu_{3.5}Al_{1.5}$ and indicates the logarithmic temperature dependence.
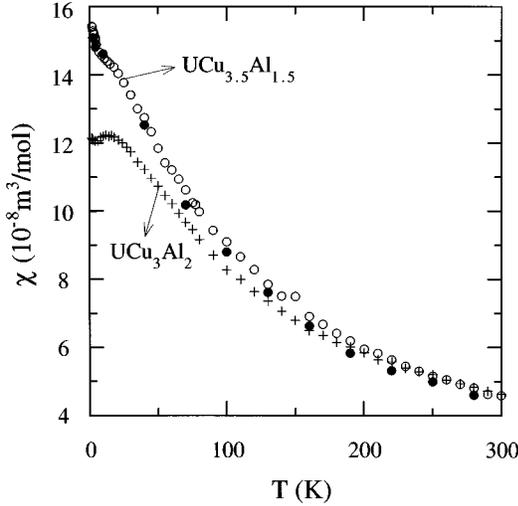
FIG. 4. Temperature dependence of the magnetic susceptibility of polycrystalline $UCu_{3.5}Al_{1.5}$ ($\bigcirc$) and UCu_3Al_2 (+). The solid circles represent the M/H values of $UCu_{3.5}Al_{1.5}$ in an applied field of 18 T.

FIG. 5. Temperature dependence of the magnetic susceptibility of polycrystalline $UCu_{3.5}Al_{1.5}$ ($\bigcirc$) and UCu_3Al_2 (+) in a log-log representation. The dashed line represents a fit of the low-temperature susceptibility of $UCu_{3.5}Al_{1.5}$ to a function of the form $a + bT^{-1/3}$. In the plot, there are also included the results of single-crystalline UCu_3Al_2 (solid lines) for $\mathbf{B} \perp c$ and $\mathbf{B} \| c$.

field of 5 T. For higher temperatures ($T > 15$ K), C/T of $UCu_{3.5}Al_{1.5}$ is enhanced by about 70 mJ/K^2 mol compared to UCu_3Al_2. This may indicate a larger electronic contribution to the specific heat in the former compound.

B. Magnetic susceptibility

Between 1.4 and 300 K, the magnetic response of $UCu_{3.5}Al_{1.5}$ and UCu_3Al_2 in fields up to 1.3 T was measured by means of a pendulum magnetometer. At all temperatures, linear magnetization curves were found and we can therefore identify the magnetic susceptibility as the slope of the M vs H curve.

The results are shown in Fig. 4. UCu_3Al_2 exhibits a broad maximum slightly above 10 K, which is close to the temperature of the specific-heat maximum. For $UCu_{3.5}Al_{1.5}$, we find a flattening of the susceptibility around 20 K, which is followed by a strong divergence at lower temperatures. Above 50 K, we find Curie-Weiss behavior for both compounds with effective moments close to the free-ion values of U^{3+} or U^{4+} ($\approx 3.6\mu_B$). We have checked the field dependence of the magnetization of $UCu_{3.5}Al_{1.5}$ up to 18 T, at various temperatures, using a vibrating-sample magnetometer in the 20-T superconducting magnet at the Pulsed Field Facility of the NHMFL at Los Alamos National Laboratory. Up to the highest field applied, we find linear magnetizations at all temperatures. The M/H values at 18 T of $UCu_{3.5}Al_{1.5}$ have been included as solid circles in Fig. 4.

Using a log-log representation in Fig. 5, we show the magnetic susceptibility of both polycrystals $UCu_{3.5}Al_{1.5}$ and UCu_3Al_2 (symbols in Fig. 5) and the single-crystal results on UCu_3Al_2 (solid lines in Fig. 5). We find that the low-temperature part of the susceptibility of $UCu_{3.5}Al_{1.5}$ is well described by a function of the form $a + bT^{-1/3}$ (dashed line in Fig. 5). Scaling of $\chi_0 \propto T^{-1/3}$ was reported also for the non-Fermi-liquid compound $UCu_{3.5}Pd_{1.5}$.[15] Here, however, we find that the low-temperature susceptibility consists out of temperature-independent and temperature-dependent
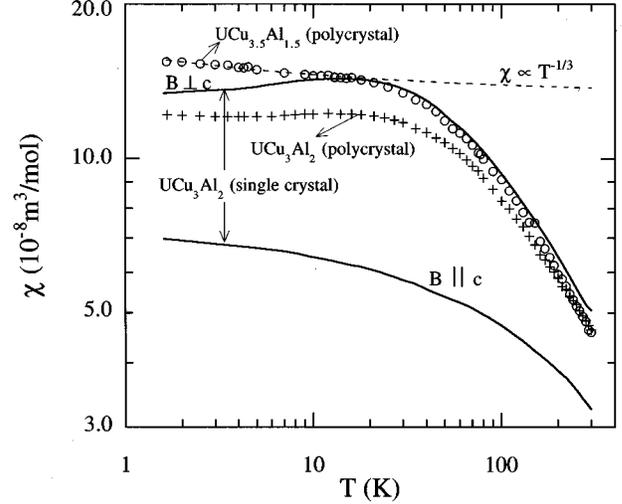
(showing $T^{-1/3}$ scaling) contributions. This may indicate that both Fermi-liquid and non-Fermi-liquid contributions occur in the polycrystalline average. The magnetic susceptibility of polycrystalline UCu_3Al_2, on the other hand, does not show a temperature dependence expected for non-Fermi-liquid materials. However, comparison with the single-crystal results on UCu_3Al_2 clearly shows that any temperature dependence seen in polycrystals may be due to averaging anisotropic response over all crystallographic directions. While magnetic interactions dominate the response within the hexagonal basal plane and give rise to the maximum in the magnetic susceptibility, we find very different behavior for fields applied along the c axis. The c-axis susceptibility is not only much weaker, but also shows very different behavior at low temperatures. In fact, we find that the c-axis susceptibility of UCu_3Al_2 diverges at low temperatures. This might imply that the c-axis susceptibility of UCu_3Al_2 shows traces of non-Fermi-liquid scaling, while magnetic correlations dominate the in-plane response. Note that only the interplanar interactions in this compound are affected by structural disorder, which may indicate that disorder is an essential ingredient for non-Fermi-liquid behavior in these compounds.

C. High-field magnetization

High-field-magnetization measurements on $UCu_{3.5}Al_{1.5}$ and UCu_3Al_2 were performed in the Amsterdam High-Field Facility. At this facility, controlled high-field pulses allow measurements of the magnetic response at any desired field shape within the fairly broad design limitations. Magnetization measurements up to 35 T are usually done in stepwise pulses, where fields are kept constant (within 3 mT) for at least 80 ms. In this way, the effect of eddy-current shielding in metallic samples can be minimized.

The magnetizations of $UCu_{3.5}Al_{1.5}$ and UCu_3Al_2 were measured on powdered particles (with a size smaller than
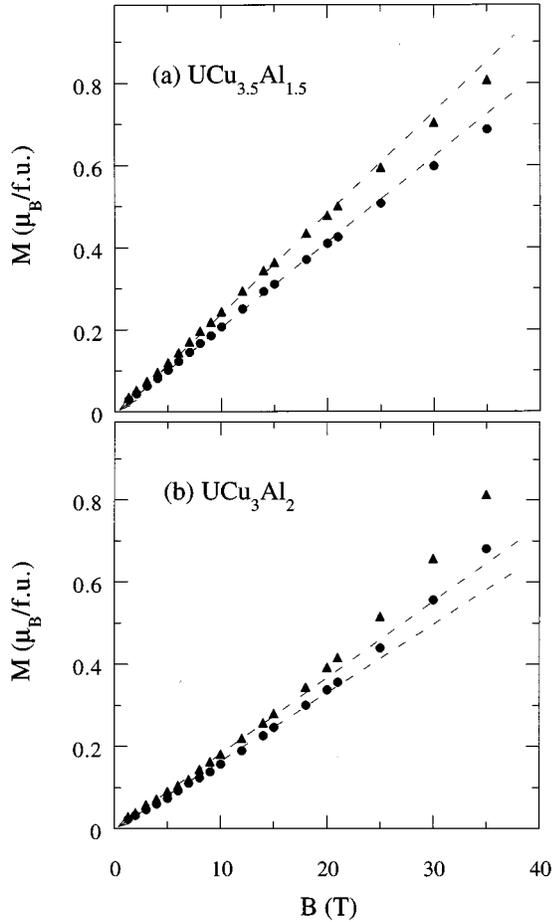
FIG. 6. Field dependence of the magnetization of polycrystalline (a) $UCu_{3.5}Al_{1.5}$ and (b) UCu_3Al_2 measured as ''free powder'' (▲) and ''fixed powder'' (●), respectively (see text). Note the apparent difference in the free- and fixed-powder results. The dashed lines are guides to the eye and show the deviation from linearity in the magnetic response of both compounds.

FIG. 7. Field dependence of the magnetization of single-crystalline UCu_3Al_2 for $\mathbf{B}\perp c$ (○) and $\mathbf{B}\|c$ (△). The symbols represent the data obtained in step wise pulses (see text), whereas the solid lines represent the result obtained in field sweeps with continuously changing field.

The results of the high-field-magnetization experiments (up to 38 T) on single-crystalline UCu_3Al_2 confirm a multiaxial type of anisotropy (see Fig. 7). At 4.2 K, the magnetization exhibits a slight S shape for fields within the basal plane, similar to the results for the heavy-fermion superconductor UPt_3.[17] At the highest field (38 T), the magnetization is a little greater than $1\mu_B$/f.u. The c-axis response is much weaker, and we find values slightly above $0.3\mu_B$/f.u. in 38 T. Furthermore, there is no S-shape behavior along this direction.

D. Electrical resistivity

Between 300 mK and 300 K, the electrical resistivities were measured on two bar-shaped polycrystals of $UCu_{3.5}Al_{1.5}$ and UCu_3Al_2 using the standard four-point ac technique. The contacts were established using silver paint. As some small cracks were present in both samples, no accurate determination of absolute resistivity values was possible. Therefore, the resistivity values were normalized to the room-temperature values.

The relative temperature dependences of the electrical resistivity of $UCu_{3.5}Al_{1.5}$ and UCu_3Al_2 are shown in Fig. 8 plotted against $\log T$. Both are very unusual. Upon cooling from room temperature, the electrical resistivity of $UCu_{3.5}Al_{1.5}$ first increases with lowering temperature; then, it goes through a maximum around 30 K. At low temperatures, there is no evidence for a linear temperature dependence, the form that is often found in non-Fermi-liquid materials. Fermi-liquid behavior, on the other hand, is expected to display a T^2 dependence, which is clearly not observed. As shown in Fig. 8, fitting of the low-temperature part of $\rho(T)$ for $UCu_{3.5}Al_{1.5}$ implies a $T^{2/3}$ temperature scaling. One should, however, not overinterpret the exponent of 2/3 as the polycrystalline average of the anisotropic properties may, as was argued for the magnetic susceptibility, result in a peculiar temperature dependence.

100 μm) both free to be oriented by the applied field and in random orientations fixed by frozen alcohol. The former result (''free powder'') is believed to represent the magnetic response along the easy magnetization direction, while the latter result (''fixed powder'') simulates an ''ideal'' polycrystal. The difference between the free-powder and fixed-powder magnetizations can be taken as a measure of the magnetic anisotropy.

In Fig. 6, the free-powder and fixed-powder results for $UCu_{3.5}Al_{1.5}$ and UCu_3Al_2 at 4.2 K in fields up to 35 T are shown. While the magnetization curves of UCu_3Al_2 display a pronounced upturn at fields above 15 T, the opposite tendency is observed for $UCu_{3.5}Al_{1.5}$ above 30 T. At somewhat higher fields, some slight saturation tendency has been observed also for UCu_3Al_2, but, even in 50 T, no full saturation is achieved in either compound $UCu_{3.5}Al_{1.5}$ and UCu_3Al_2.[10] For all fields, a higher response of the free-powder magnetization is seen in $UCu_{3.5}Al_{1.5}$ compared to UCu_3Al_2, which may indicate a larger saturated moment for the former compound. For both compounds, we find that the ratios of M_{fix}/M_{free} at 35 T are larger than 0.8, which is indicative of multiaxial-type anisotropy in both compounds.[16]

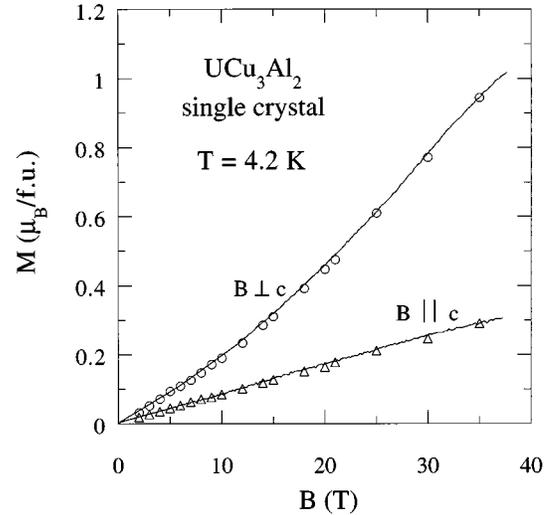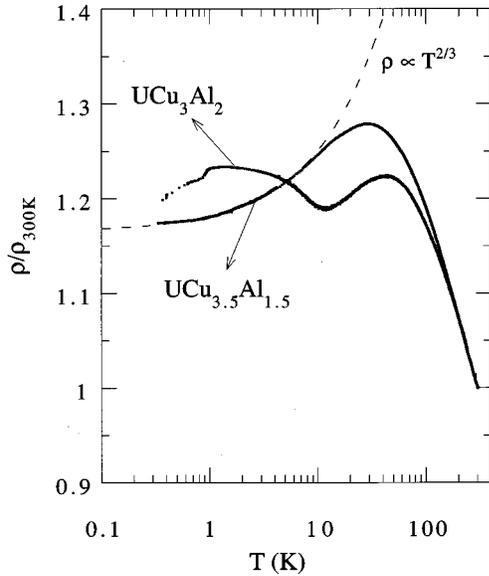FIG. 8. Temperature dependences of the electrical resistivities of $UCu_{3.5}Al_{1.5}$ and UCu_3Al_2 normalized to their room-temperature values. Note the logarithmic temperature scale. The dashed line represents a fit of the low-temperature resistivity of $UCu_{3.5}Al_{1.5}$ to a function of the form $a+bT^{2/3}$.

Down to about 10 K, the overall shape of the electrical resistivity of UCu_3Al_2 is very similar to that of $UCu_{3.5}Al_{1.5}$. At this temperature, a minimum occurs in the electrical resistivity, and this coincides with the maxima in the temperature dependences of the specific heat and the magnetic susceptibility. Upon further lowering of the temperature, some saturation tendency is observed, but around 800 mK there is a sudden drop in electrical resistivity. At present, we have little idea about the origin of this anomaly. However, there is no evidence of an anomaly at this temperature in other bulk properties (e.g., in the specific heat), and therefore we doubt that it is intrinsic to UCu_3Al_2. It might be due to some small amount of some impurity phase (U_2Cu_9Al or elemental Al).

IV. NEUTRON-DIFFRACTION RESULTS

Our previous neutron-diffraction studies[11] were restricted to powders of UCu_3Al_2, and the results gave the crystal structure shown in Fig. 1. At low temperature, no additional magnetic peaks were observed, and an upper limit of $0.4\mu_B$ for the size of any ordered moment at low temperatures was estimated.[11]

In this paper we discuss the crystal structure of $UCu_{3.5}Al_{1.5}$ measured by neutron powder diffraction, and we also looked for magnetic moments smaller than $0.4\mu_B$ in UCu_3Al_2 by neutron diffraction on a single crystal.

A. Neutron powder diffraction on $UCu_{3.5}Al_{1.5}$

For the neutron-diffraction experiments, about 7 g of $UCu_{3.5}Al_{1.5}$ were ground and enclosed under He atmosphere in a sealed vanadium can. This can was mounted on the cold finger of a displex refrigerator, which in turn was mounted on the Neutron Powder Diffractometer (NPD) at the Manuel
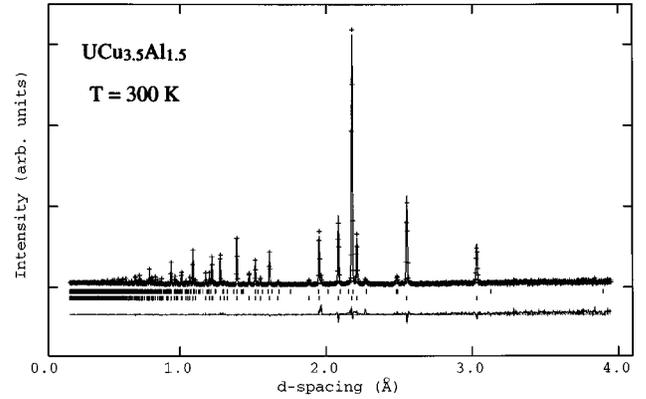

FIG. 9. Observed and calculated nuclear structure profile of $UCu_{3.5}Al_{1.5}$ at 300 K, as measured on the $+90°$ bank of NPD. Starting from the bottom, the reflection markers denote $UCu_{3.5}Al_{1.5}$ (with parameters as given in Table I) and U_2Cu_9Al. The difference of measured and calculated intensities is shown by the solid line below. The intensities have been divided by the incident spectrum.

Lujan Jr. Neutron Scattering Center, Los Alamos National Laboratory. The NPD currently has four banks of detectors at $±90°$ and $±148°$. Data were taken at 300 and 12 K, and we collected data for about 12 h at each temperature. The diffraction patterns were analyzed using the Rietveld refinement program GSAS,[18] which allows simultaneous refinement of multiple phases.

Our data rule out complete disorder of Cu and Al atoms (reduced $\chi^2=6.991$ as opposed to $\chi^2=4.768$ for the structure in Fig. 1), which had previously been proposed for this compound.[10] As in UCu_3Al_2, we find for $UCu_{3.5}Al_{1.5}$ that the $2c$ positions are occupied by Cu atoms only, while a statistical distribution of Al and the remaining Cu atoms is found on the $3g$ sites. Not only do we find a lower χ^2 for this structure, but refining the fractional occupancies on the $2c$ and $3g$ positions converges to Cu and Al occupancies close to those given in Table I, though a somewhat higher Al fraction ($=0.56±0.02$) is derived for the $3g$ sites. We also checked for slight distortions and displacements of the atoms involving a cell doubling, but the absence of any superlattice reflections does not support this. Therefore, the diffraction patterns of $UCu_{3.5}Al_{1.5}$ are well described assuming the same crystal structure as for UCu_3Al_2 (see Fig. 1). A few reflections in the diffraction pattern remain unindexed if one assumes that $UCu_{3.5}Al_{1.5}$ is the only phase. As can be seen in Fig. 9, the diffraction pattern is fully described if the refinement includes some 2% vol. of the Cu-rich ternary, U_2Cu_9Al (space group $P6_3/mmc$).[14] The least-squares refinements including all four banks yield lattice parameters and R factors as given in Table I.

B. Neutron diffraction on single-crystalline UCu_3Al_2

We also performed neutron-diffraction experiments on a single crystal of UCu_3Al_2 in order to clarify the origin of an anomaly, which appears near 10 K, in the temperature dependencies of the magnetic susceptibility, the electrical resistivity, and the specific heat. For this purpose, we have

collected diffraction patterns on the Single Crystal Diffractometer (SCD) at the Intense Pulsed Neutron Source at Argonne National Laboratory. The single crystal of UCu_3Al_2 was mounted on the sample holder of a Heli-Tran Liquid Transfer Refrigeration System, which allows measurements in the temperature range between 2 and 300 K. Data were taken at 20 K (5 histograms) and 6 K (11 histograms), above and below the presumed magnetic-ordering temperature. Each histogram was counted for about 3 h.

Compared to the 20-K data, there are no additional peaks at 6 K, which would be of magnetic origin. Also a triangular coplanar configuration of the moments, which gives magnetic contributions on the nuclear Bragg reflections only,[19] is not supported by our data. Assuming a variety of different magnetic configurations, our data indicate that any ordered moment must be less than $0.1\mu_B$.

V. CONCLUSIONS

At low temperatures, the bulk properties of neither $UCu_{3.5}Al_{1.5}$ nor UCu_3Al_2 show the temperature dependences predicted by Fermi-liquid theory. The specific heat of $UCu_{3.5}Al_{1.5}$ diverges logarithmitically, which is evidence for non-Fermi-liquid scaling. The other properties are somewhat ambiguous in their temperature dependences because the magnetic anisotropy contributes differently to different crystallographic directions. Nevertheless, if the anisotropy effects are taken into account correctly, one may check for internal consistency of the critical exponents. Given the exponent of $-1/3$ in $\chi(T)$, multichannel impurity models give an exponent of $1/3$ for ρ,[20] while spin-fluctuation theory provide some mechanism that correctly predicts the observed exponent of $2/3$ in ρ.[21] This may support the idea that the $T=0$ phase transition in question is three dimensional in character (and not impuritylike as in $UCu_{5-x}Pd_x$). UCu_3Al_2 behaves similar to $UCu_{3.5}Al_{1.5}$, albeit with the superposition of an anomaly at around 8–10 K.

The present neutron-diffraction results show no difference in the crystal structures of $UCu_{3.5}Al_{1.5}$ and UCu_3Al_2, which is surprising given the irregular composition dependence of the lattice parameters (see Fig. 2). Very small displacements and/or distortions cannot be excluded on the basis of our powder diffraction data, and single-crystal studies are needed to confirm this conclusion. On the other hand, intensity-analysis results clearly exclude a completely random distribution of Cu and Al atoms for both compounds. Randomness in $UCu_{3.5}Al_{1.5}$ and UCu_3Al_2 is restricted to the $3g$ positions located on the intermediate planes between U-containing planes of the $CaCu_5$ structure. Therefore, only interplanar interactions are affected by the disorder. This provides a new perspective on non-Fermi-liquid scaling because structural randomness is an essential ingredient in many scenarios sug-

gested for the understanding of non-Fermi-liquid behavior. Non-Fermi-liquid scaling due to a distribution of Kondo temperatures because of disorder has been invoked, e.g., in $U(Cu,Pd)_5$ compounds,[22] and this disorder is believed to be a direct consequence of the random distribution of Cu and Pd atoms.

The origin of the anomalies in the bulk properties of UCu_3Al_2 remains a mystery. No magnetic Bragg peaks have been observed, and an upper limit for the ordered moment of $0.1\mu_B$ has been estimated. At present, we do not know whether the observed anomalies in bulk investigations reflect long-range order of even smaller magnetic moments or whether they should be attributed to other correlation effects, e.g., spin-glass behavior. The proximity to a spin-glass state has been argued for many non-Fermi-liquid systems, and there is indeed strong evidence for a spin glass in compounds with a diluted f-electron sublattice, for example, in $U_{0.6}Y_{0.4}Pd_3$.[23] In UCu_3Al_2, however, there is no randomness on the f-electron sublattice. Such a periodic arrangement of magnetic atoms is not a favorable situation for formation of a spin-glass state.[24] The huge observed magnetic anisotropy may be taken as further evidence against a three-dimensional spin glass.[25] On the other hand, interactions between the planes are driven by a *Kagomé* net of statistically distributed Cu and Al atoms. If interplane interactions are dominant compared to intraplane interactions, this might indeed lead to a complex arrangement of the moments in two dimensions. Sensitive local probes like muon spin resonance (μSR) might be able to clarify this.

Up to now, most of the non-Fermi-liquid materials known in the literature have not been studied in single crystalline form. Our single-crystal studies on UCu_3Al_2 indicate that a huge magnetic anisotropy is present in the $U(Cu,Al)_5$ system. The role of possible magnetic anisotropy is ambiguous for non-Fermi-liquid materials which form in low-symmetry crystallographic structures, like $(U,Th)Ru_2Si_2$ and $(U,Th)Pd_2Al_3$.[3] For an appropriate account of the anisotropy in such systems, single crystals are indispensable. Therefore, we intend to concentrate on single crystals for future studies of the $U(Cu,Al)_5$ system.

ACKNOWLEDGMENTS

[1] For a recent review, see F. Steglich, C. Geibel, K. Gloos, G. Olesch, C. Schank, C. Wassilew, A. Loidl, A. Krimmel, and G. R. Stewart, J. Low Temp. Phys. **95**, 3 (1994).

[2] H. v. Löhneysen, Physica B **206&207**, 101 (1995).

[3] M. B. Maple, C. L. Seaman, D. A. Gajewski, Y. Dalichaouch, V.

B. Barbetta, M. C. de Andrade, H. A. Mook, H. G. Lukefahr, O. O. Bernal, and D. E. MacLaughlin, J. Low Temp. Phys. **95**, 225 (1994).

[4] C. L. Seaman, M. B. Maple, B. W. Lee, S. Chamaty, M. S. Torikachvili, J. S. Kang, L. Z. Liu, J. W. Allen, and D. L. Cox,

Phys. Rev. Lett. **67**, 2882 (1991).

[5] B. Andraka and A. M. Tsvelik, Phys. Rev. Lett. **67**, 2886 (1991).

[6] H. Amitsuka, T. Hidano, T. Honma, H. Mitamura, and T. Sakakibara, Physica B **186-188**, 337 (1993).

[7] H. v. Löhneysen, T. Pietrus, G. Portisch, H. G. Schlager, A. Schröder, M. Sieck, and T. Trappmann, Phys. Rev. Lett. **72**, 3262 (1994).

[8] B. Andraka and G. R. Stewart, Phys. Rev. B **47**, 3208 (1993).

[9] M. C. Aronson, R. Osborn, R. A. Robinson, J. W. Lynn, R. Chau, C. L. Seaman, and M. B. Maple, Phys. Rev. Lett. **75**, 725 (1995).

[10] H. Nakotte, K. H. J. Buschow, J. C. P. Klaasse, K. Prokeš, F. R. de Boer, A. V. Andreev, K. Sugiyama, T. Kuroda, and M. Date, J. Magn. Magn. Mater. **140-144**, 1261 (1995).

[11] H. Nakotte, E. Brück, J. H. V. J. Brabers, K. Prokeš, F. R. de Boer, V. Sechovsky, K. H. J. Buschow, A. V. Andreev, R. A. Robinson, A. Purwanto, and J. W. Lynn, IEEE Trans. Magn. **MAG-30**, 1217 (1994).

[12] C. Geibel, S. Thies, D. Kaczorowski, A. Mehner, A. Grauel, B. Seidel, U. Ahlheim, R. Helfrich, K. Petersen, C. D. Bredl, and F. Steglich, Z. Phys. B **83**, 305 (1991); C. Geibel, C. Schank, S. Thies, H. Kitazawa, C. D. Bredl, A. Böhm, M. Rau, A. Grauel, R. Caspary, R. Helfrich, U. Ahlheim, G. Weber, and F. Steglich, *ibid*. **84**, 1 (1991).

[13] The term *Kagomé* comes from the Japanese art of folding paper, origami. It refers specifically to a certain type of two-dimensional lattice constructed from corner-shared triangular units [see, for example, J. N. Reimers, A. J. Berlinsky, and A. C. Shi, Phys. Rev. B **43**, 865 (1991)]. Such *Kagomé* lattices are prone to highly frustrated magnetic behavior [see, for example, G. Aeppli *et al.*, Physica B **213&214**, 142 (1995)].

[14] Ž. Blažina and Z. Ban, Z. Naturforsch, **28**, 561 (1973).

[15] B. Andraka, Physica B **199−200**, 239 (1994).

[16] H. Nakotte, K. Bakker, Z. Koziol, F. R. de Boer, and A. V. Andreev, IEEE Trans. Magn. **MAG-30**, 1199 (1994).

[17] P. H. Frings, J. J. M. Franse, F. R. de Boer, and A. Menovsky, J. Magn. Magn. Mater. **31-34**, 240 (1983).

[18] A. C. Larson and R. B. Von Dreele, Los Alamos National Laboratory Report, No. LA-UR-86-748.

[19] A. Purwanto, R. A. Robinson, K. Prokeš, H. Nakotte, F. R. de Boer, L. Havela, V. Sechovsky, N. C. Tuan, Y. Kergadallan, J. C. Spirlet, and J. Rebizant, J. Appl. Phys. **76**, 7040 (1994).

[20] I. Affleck and A. W. W. Ludwig, Phys. Rev. B **48**, 7297 (1993).

[21] A. B. Kaiser and S. Doniach, Int. J. Magn. **1**, 11 (1970).

[22] O. O. Bernal, D. E. MacLaughlin, H. G. Lukefahr, and B. Andraka, Phys. Rev. Lett. **75**, 2023 (1995).

[23] M. A. Lopez de la Torre, J. Rodriguez Fernandez, and K. A. McEwen, J. Appl. Phys. **79**, 6364 (1996).

[24] J. Chappert, in *Magnetism of Metals and Alloys*, edited by M. Cyrot (North-Holland, Amsterdam, 1982).

[25] K. Moorjani and J. M. D. Coey, *Magnetic Glasses* (Elsevier, Amsterdam, 1984).